Influence of Shell Geometry on Buckling Optimization of Fiber-Composite Laminate Shells

H.-T. Hu

Research Engineer,
National Center for Composite Materials
Research,
University of Illinois,
Urbana, Ill. 61801
Assoc. Mem. ASME

The buckling strength of fiber-composite laminate shells with given loading condition and material system is maximized with respect to fiber orientations by using a sequential linear programming method together with a simple move-limit strategy. Significant influence of shell thickness and shell length on the optimal fiber angles, the critical buckling loads and the critical buckling modes of fiber-composite laminate shells has been shown through this investigation.

Introduction

Applications of fiber-composite materials (Fig. 1) to advanced shell structures such as aircraft fuselages, deep submersibles and surface ships have been increased rapidly in recent years. These composite laminate shells in service are commonly subjected to various kinds of external loading. Structural instabi'ity becomes a major concern in safe and reliable design of the advanced composite shells. The buckling strength of fiber-composite structures depends on various lamination parameters such as ply orientations (Onoda, 1985; Sun and Hansen, 1988; Jun and Hong, 1988; Hu and Wang, 1990), and geometric variables, such as structural configurations and dimensions (Whitney, 1984; Knight and Starnes, 1985; Jun and Hong, 1988). Therefore, proper selection of appropriate lamination and geometric variables for a given composite material system to realize its maximum structural buckling strength becomes a crucial problem.

Research on the subject of structural optimization has been reported by many investigators (Schmit, 1981). However, applications of optimization methods to stability analysis and design of complex fiber-composite shell structures have been very limited. Among various optimization schemes, sequential linear programming methods have been successfully applied to many large-scale structural problems (Zienkiewicz and Champbell, 1973; Vanderplatts, 1984). Linearization of nonlinear optimization problems to meet requirements for iterative applications of a linear programming method is one of the most popular approaches to solve the structural optimization problem.

In this investigation, buckling optimization of fiber-composite laminate shell with respect to fiber orientations is solved by using a sequential linear programming method together with a simple move-limit strategy. The critical buckling loads of composite shells are calculated by the linearized buckling analysis implemented in ABAQUS finite element program (Hibbitt, Karlsson and Sorensen, 1990). In this paper, the linearized buckling analysis and optimization method are briefly reviewed

first. Then the influence of shell thickness and length on the optimal fiber orientations, the critical buckling loads and the critical buckling modes of composite shells is presented. Finally, important conclusions obtained from the study are given.

Linearized Buckling Analysis

In the finite-element modeling scheme for spatial discretization, a system of nonlinear algebraic equations results in the incremental form

$$[K]_t d\{U\} = d\{P\} \qquad (1)$$

where $\{K\}_t$ is the tangent stiffness matrix, $d\{U\}$ the incremental nodal displacement vector, and $d\{P\}$ the incremental nodal force vector.

Assuming that the linear theory of small deformation before buckling holds, the terms which are functions of nodal displacements in the general nonlinear tangent stiffness matrix can be neglected. The linearized formulation then gives rise to a tangent stiffness matrix with the following expression (Cook, Malkus and Plesha, 1989):
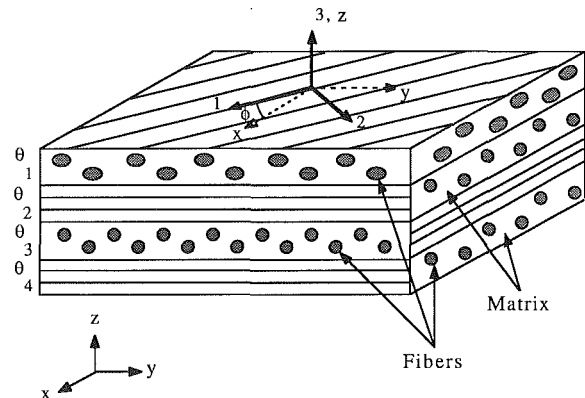
$$[K]_t = [K]_L + [K]_\sigma \qquad (2)$$

Fig. 1 Material and element coordinate systems for fiber-composite laminate

where $[K]_L$ is a linear stiffness matrix, and $[K]_\sigma$ a geometric stiffness matrix dependent upon stresses.

The bifurcation solution for the linearized buckling problem may be determined from the following eigenvalue equation:

$$([K]_L + \lambda[K]_{\sigma_o})\{\psi\} = \{0\} \tag{3}$$

where λ is an eigenvalue, and $\{\psi\}$ an eigenvector. The critical load P_{cr} can be found from $P_{cr} = \lambda P_o$ where P_o is the nominal load which corresponds to the stress state σ_o. A subspace iteration procedure (Bathe and Wilson, 1972) is used in ABAQUS to solve for the eigenvalues and eigenvectors.

Sequential Linear Programming

A general optimization problem may be defined as the following:

$$\text{Minimize:} \quad f(\mathbf{x}) \tag{4a}$$
$$\text{Subjected to:} \quad g_i(\mathbf{x}) \le 0, \ i = 1, \ldots, r \tag{4b}$$
$$h_j(\mathbf{x}) = 0, \ j = r+1, \ldots, m \tag{4c}$$
$$p_k \le x_k \le q_k, \ k = 1, \ldots, n \tag{4d}$$

where $f(\mathbf{x})$ is an objective function, $g_i(\mathbf{x})$ are inequality constraints, $h_j(\mathbf{x})$ are equality constraints, and $\mathbf{x} = \{x_1, x_2, \ldots, x_n\}^T$ is a vector of design variables. If a particular optimization problem requires maximization, we simply minimize $-f(\mathbf{x})$.

For the general optimization problem of Eqs. $(4a)-(4d)$, a linearized problem may be constructed by approximating the nonlinear functions about a current solution point, $\mathbf{x}_o = \{x_{o1}, x_{o2}, \ldots, x_{on}\}^T$, in a first-order Taylor series expansion as follows:

$$\text{Minimize:} \quad f(\mathbf{x}) \approx f(\mathbf{x}_o) + \nabla f(\mathbf{x}_o)^T \delta\mathbf{x} \tag{5a}$$
$$\text{Subjected to:} \quad g_i(\mathbf{x}) \approx g_i(\mathbf{x}_o) + \nabla g_i(\mathbf{x}_o)^T \delta\mathbf{x} \le 0 \tag{5b}$$
$$h_j(\mathbf{x}) \approx h_j(\mathbf{x}_o) + \nabla h_j(\mathbf{x}_o)^T \delta\mathbf{x} = 0 \tag{5c}$$
$$p_k \le x_k \le q_k \tag{5d}$$

where $i = 1, \ldots, r; \ j = r + 1, \ldots, m; \ k = 1, \ldots, n;$ $\delta\mathbf{x} = \{x_1 - x_{o1}, x_2 - x_{o2}, \ldots, x_n - x_{on}\}^T$.

It is clear that Eqs. $(5a)-(5d)$ represent a linear programming problem where variables are contained in the vector $\delta\mathbf{x}$. A solution for Eqs. $(5a)-(5d)$ may be easily obtained by the simplex method (Kolman and Beck, 1980). After obtaining an initial approximate solution for Eqs. $(5a)-(5b)$, say x_1, we can linearize the original problem, Eqs. $(4a)-(4d)$, at x_1 and solve the new linear programming problem. The process is repeated until a precise solution is achieved. This approach is referred to as sequential linear programming (Zienkiewicz and Champbell, 1973; Vanderplatts, 1984).

Although the procedure for a sequential linear programming is simple, difficulties may arise during the iterations. First, the optimum solution for the approximate linear problem may violate the constraint conditions of the original optimization problem. Second, in a nonlinear problem, the true optimum solution may appear between two constraint intersections. A straightforward successive linearization in such a case may lead to an oscillation of the solution between the widely separated values. Difficulties in dealing with such a problem may be avoided by imposing a "move limit" on the linear approximation (Zienkiewicz and Champbell, 1973; Vanderplatts, 1984; Esping, 1984). The concept of a move limit is that a set of box-like admissible constraints are placed in the range of $\delta\mathbf{x}$. It is known that computational economy and accuracy of the approximate solution may depend greatly on the choice of the move limit. (If the move limits are made too small, solution convergence may be very slow. If they are too large, oscillations may occur.) In general, the choice of a suitable move limit depends on experience and also on the results of previous steps. Once a proper move limit is chosen at the beginning of the sequential linear programming procedure, this move limit should gradually approach zero as the iterative process continues.

The algorithm of a sequential linear programming with selected move limits may be summarized as follows:

1 Linearize the nonlinear objective function and associated constraints with respect to an initial design $\mathbf{x}_o$.

2 Impose move limits in the form of $-\mathbf{S} \le (\mathbf{x} - \mathbf{x}_o) \le \mathbf{R}$, where $\mathbf{S}$ and $\mathbf{R}$ are properly chosen positive constraints.

———— Nomenclature ————

E_{11}, E_{22} = Young's moduli for composite lamina

G_{12}, G_{13}, G_{23} = shear moduli for composite lamina

$f(\mathbf{x})$ = objective function

$g_i(\mathbf{x}), h_j(\mathbf{x})$ = inequality constraints and equality constraints

p_{cr} = critical buckling pressure

$\mathbf{x} = \{x_1, x_2, \ldots, x_n\}$ = vector of design variables

z_{jt}, z_{jb} = distance from mid-surface to top and bottom of the jth layer

α_1, α_2 = correction factors for transverse shear

λ = eigenvalue

ν_{12}, ν_{21} = Poisson's ratios for composite lamina

ϕ = rotational angle between material coordinates and element coordinates

(x, y) = element coordinates

$(1, 2)$ = material coordinates

$[K]_t, [K]_L$ = tangent and linear stiffness matrices

$[K]_\sigma, [K]_{\sigma_o}$ = geometric stiffness matrices

$[Q_1'], [Q_2']$ = material constitutive matrices in material coordinates

$[Q_1], [Q_2]$ = material constitutive matrices in element coordinates

$[T_1], [T_2]$ = transformation matrices

$\{N\}, \{M\}, \{V\}$ = vectors of stress resultants

$d\{P\}$ = incremental nodal force vector

$d\{U\}$ = incremental nodal displacement vector

$\{\epsilon_o\} = \{\epsilon_{xo}, \epsilon_{yo}, \gamma_{xyo}\}$ = in-plane strain vector at mid-surface of section

$\{\epsilon'\} = \{\epsilon_1, \epsilon_2, \gamma_{12}\}$ = in-plane strain vector in material coordinates

$\{\epsilon\} = \{\epsilon_x, \epsilon_y, \gamma_{xy}\}$ = in-plane strain vector in element coordinates

$\{\gamma_t'\} = \{\gamma_{13}, \gamma_{23}\}$ = transverse strain vector in material coordinates

$\{\gamma_t\} = \{\gamma_{xz}, \gamma_{yz}\}$ = transverse strain vector in element coordinates

$\{\kappa\} = \{\kappa_x, \kappa_y, \kappa_{xy}\}$ = vector of curvature

$\{\sigma'\} = \{\sigma_1, \sigma_2, \tau_{12}\}$ = in-plane stress vector in material coordinates

$\{\sigma\} = \{\sigma_x, \sigma_y, \tau_{xy}\}$ = in-plane stress vector in element coordinates

$\{\tau_t'\} = \{\tau_{13}, \tau_{23}\}$ = transverse stress vector in material coordinates

$\{\tau_t\} = \{\tau_{xz}, \tau_{yz}\}$ = transverse stress vector in element coordinates

$\{\psi\}$ = eigenvector

$\{\ \}, \{\ \}^T, [\ ]$ = row vector, column vector and matrix

Laminate layup:
$[\pm\theta/90_2/0]_{ns}$
$0^\circ \le \theta \le 90^\circ$

Composite shell geometry:
L = 16 in.
D = 8 in.
h = 0.005 in. (per ply)

Ply constitutive properties:
E_{11} = 20000 ksi
E_{22} = 2100 ksi
$G_{12} = G_{13}$ = 850 ksi
G_{23} = 510 ksi
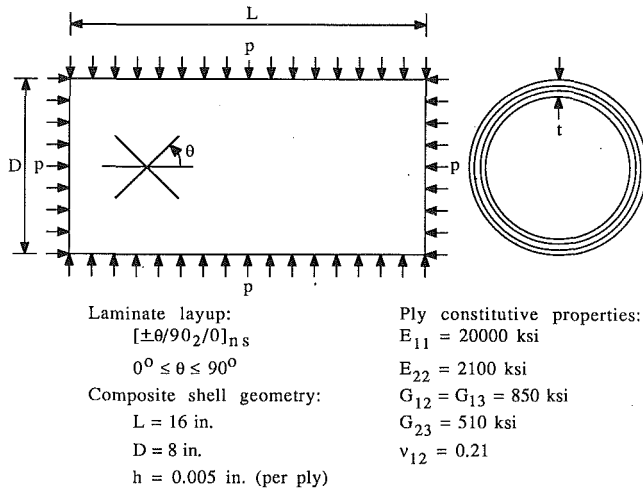v_{12} = 0.21

Note: 1 in. = 2.54 cm; 1 ksi = 6.89 Mpa

Fig. 2 Cylindrical composite laminate shell under external hydrostatic compression

3 Solve the approximate linear programming problem to obtain an initial optimum solution x_1.

4 Repeat the process by redefining x_1 with x_o until either the subsequent solutions do not change significantly (i.e., true convergence) or the move limit approaches zero (i.e., forced convergence).

Numerical Analysis

Effect of Shell Thickness on Buckling Optimization of Composite Shells. In this section, simply supported composite laminate cylindrical shells under external hydrostatic compression are investigated. The ends of these shells are closed. Hence, the pressure loads applied at two end surfaces are transformed into equivalent concentrated ring loads applied at two circular edges. All these shells have the same length, outer radius and material properties (Fig. 2). However, five different shell thicknesses are considered, i.e., shells with 20 plies ($[\pm\theta/90_2/0]_{2s}$), 40 plies ($[\pm\theta/90_2/0]_{4s}$), 60 plies ($[\pm\theta/90_2/0]_{6s}$), 80 plies ($[\pm\theta/90_2/0]_{8s}$), and 100 plies ($[\pm\theta/90_2/0]_{10s}$). The thickness of each ply is 0.005 in. (0.0127 cm). The objective of this study is to find the optimal fiber angle θ to maximize the critical buckling pressure P_{cr} of these shells and to investigate the influence of shell thickness on the optimal fiber angle, critical buckling pressure and critical buckling mode of these composite shells.

In the numerical analysis, these shells are modeled by eight-node isoparametric shell elements with six degrees of freedom per node (three displacements and three rotations). The shell formulation is based on Mindlin-type displacement field assumptions which allows transverse shear deformation (Irons, 1976). The critical buckling pressure of these shells are calculated by using the linearized buckling analysis implemented in ABAQUS. The constitutive matrix of fiber-composite laminae for the shell element is derived in Appendix I.

Based on the sequential linear programming method, in each iteration the current, linearized optimization problem becomes

Maximize: $\quad P_{cr}(\theta) \approx p_{cr}(\theta_o) + (\theta - \theta_o) \left.\dfrac{\partial p_{cr}}{\partial \theta}\right|_{\theta=\theta_o}$ $\quad$ (6a)

Subjected to: $\quad 0 \text{ deg} \le \theta \le 90 \text{ deg}$ $\quad\quad\quad$ (6b)

$\quad\quad -r \times q \times 0.5^s \le (\theta - \theta_o) \le r \times q \times 0.5^s$ $\quad$ (6c)

where θ_o is a solution in the current iteration. The r and q in Eq. (6c) are the size and the reduction rate of the move limit.
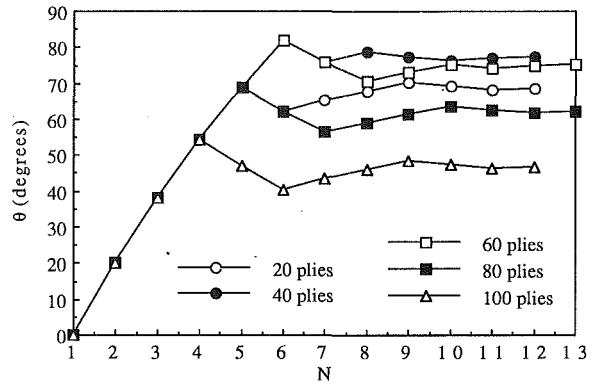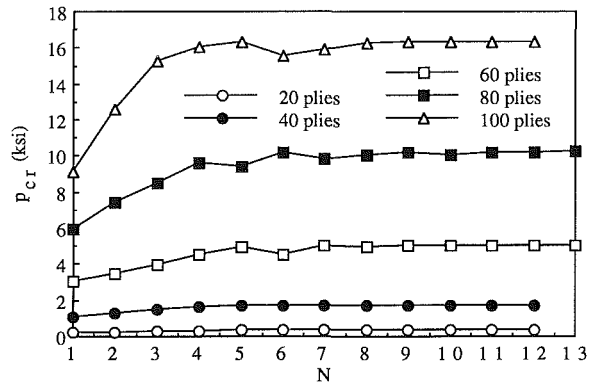

Fig. 3 Number of iterations N versus fiber orientation θ for buckling optimization of $[\pm\theta/90_2/0]_{ns}$ composite laminate shells with various thick-nesses under hydrostatic compression (simply supported ends)
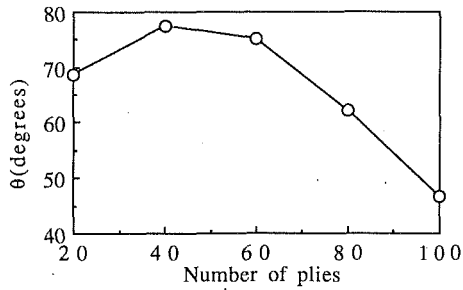

Note: 1 ksi = 6.89 Mpa

Fig. 4 Number of iterations N versus critical pressure p_{cr} for buckling optimization of $[\pm\theta/90_2/0]_{ns}$ composite laminate shells with various thick-nesses under hydrostatic compression (simply supported ends)

In the present study, the values of r and q are selected to be 20 deg and $0.9^{(N-1)}$, where N is a current iteration number. In order to control the oscillation of the solution, a parameter 0.5^s is introduced in the move limit, where s is the number of oscillations of the derivative $\partial p_{cr}/\partial \theta$ that has taken place before the current iteration. The value of s increases by 1 if the sign of $\partial p_{cr}/\partial \theta$ changes. Whenever oscillations of the solution occurs, the range of the move limit is reduced to half of its current value, which is similar to a bisection method (Maror, 1987). This expedites the solution convergent rate very rapidly.

To calculate the derivative in Eq. (6a), the $\partial p_{cr}/\partial \theta$ term may be approximated by using a forward finite-difference method with the following form:

$$\frac{\partial p_{cr}}{\partial \theta} \approx \frac{[p_{cr}(\theta_o + \Delta\theta) - p_{cr}(\theta_o)]}{\Delta\theta} \qquad (7)$$

In order to determine the value of $\partial p_{cr}/\partial \theta$ in Eq. (7) numerically, two buckling analyses are needed to compute $p_{cr}(\theta_o)$ and $p_{cr}(\theta_o + \Delta\theta)$ in each iteration. In this study, the value of $\Delta\theta$ is selected to be 1 deg in most iterations.

. Important numerical results obtained in optimization study are given in Figs. 3 and 4, which show the fiber orientation θ and the associated critical buckling pressure p_{cr} determined in each iteration for all shells. The initial values of θ are selected to be 0 deg for all composite shells. All the solutions converged within 12 or 13 iterations. Figure 5 shows the optimal fiber angles and the associated critical buckling pressure for all shells. From Fig. 5 (a) we can see that for different shell thicknesses, the values of the optimal fiber angles vary between 46.7 and 77.3 deg and the optimal fiber angle θ seems to be a second-

(a) Number of plies vs. optimal fiber orientation θ
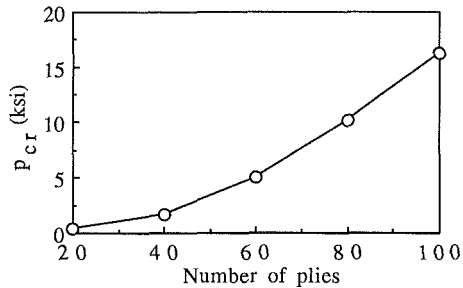
(b) Number of plies vs. critical pressure p_{cr}

Note: 1 ksi = 6.89 Mpa

Fig. 5 Effect of shell thickness on buckling optimization of $[\pm\theta/90_2/0]_{ns}$ composite laminate shells under hydrostatic compression (simply supported ends)

Critical buckling mode for shell with 20 plies
p_{cr} = 0.36 ksi (2.48 Mpa)

Critical buckling mode for shell with 100 plies
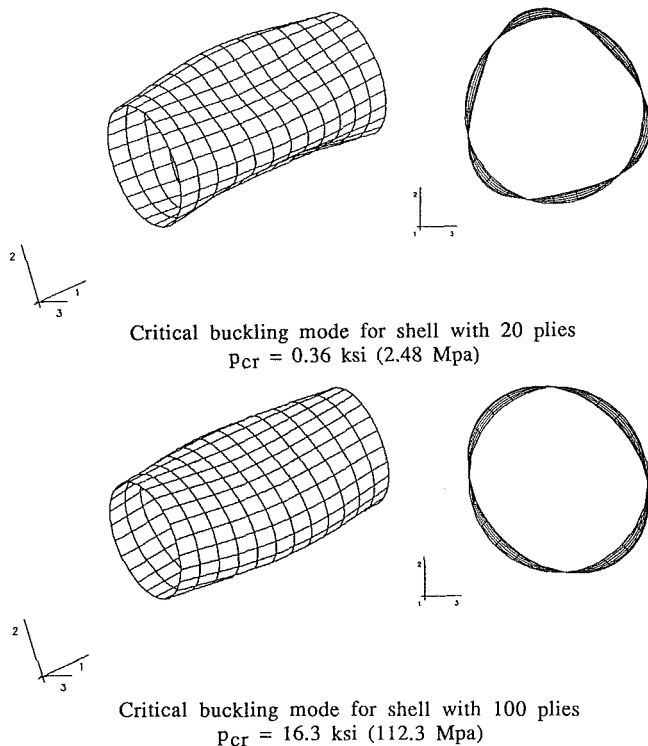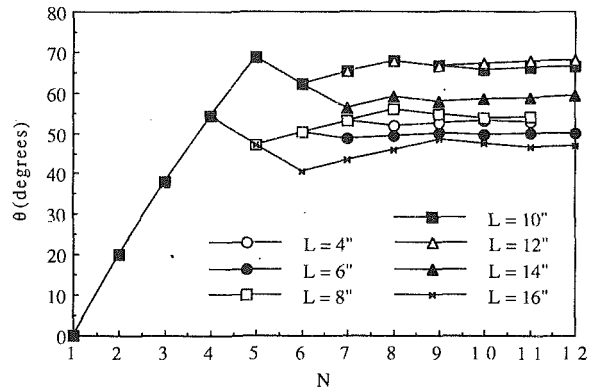p_{cr} = 16.3 ksi (112.3 Mpa)

Fig. 6 Buckling modes of $[\pm\theta/90_2/0]_{2s}$ and $[\pm\theta/90_2/0]_{10s}$ composite shells subjected to hydrostatic compression under optimal fiber orientation (simply supported ends)

order function of shell thickness. From Fig. 5(b) we can see that when the thickness of the shell section increases, the critical buckling pressure for composite shell under optimal fiber orientation increases significantly. For example, when shell thickness increases 5 times from 20 plies to 100 plies, the critical

Fig. 7 Number of iterations N versus fiber orientation θ for buckling optimization of $[\pm\theta/90_2/0]_{10s}$ composite laminate shells with various lengths under hydrostatic compression (simply supported ends)
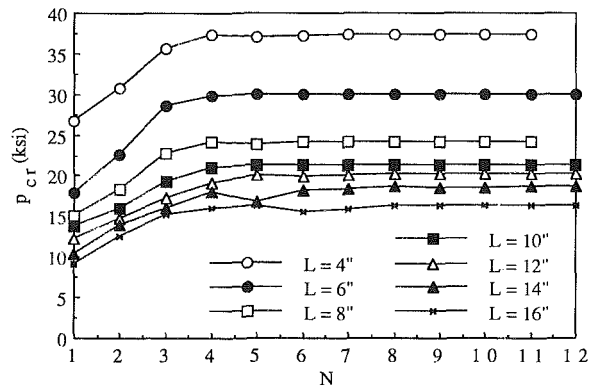
Note: 1 in. = 2.54 cm; 1 ksi = 6.89 Mpa

Fig. 8 Number of iterations N versus critical pressure p_{cr} for buckling optimization of $[\pm\theta/90_2/0]_{10s}$ composite laminate shells with various lengths under hydrostatic compression (simply supported ends)

buckling increases 45 times from 0.36 ksi (2.48 Mpa) to 16.3 ksi (112.3 Mpa). Figure 6 shows the buckling modes of composite shells under optimal fiber angles with 20 and 100 plies. All these shells buckle into a single half-wave in the longitudinal direction. However, when the thickness of the shell section increases, the buckling mode of the shell develops less surface distortion in the circumferential direction.

Effect of Shell Length on Buckling Optimization of Composite Shells. In this section, simply supported composite shells same as those in previous section but with various lengths, i.e., L equal to 4 in. (10.16 cm), 6 in. (15.24 cm), 8 in. (20.32 cm), 10 in. (25.4 cm), 12 in. (30.48 cm), 14 in. (35.56 cm) and 16 in. (40.64 cm), are investigated. All shells have the same ply layup $[\pm\theta/90_2/0]_{10s}$ and total thickness 0.5 in. (1.27 cm). The objective of this study is to find the optimal fiber angle θ to maximize the critical buckling pressure p_{cr} of these shells and to investigate the influence of shell length on the optimal fiber, critical buckling pressure and critical buckling mode of these composite shells.

The linearized optimization problem can be posted exactly the same as that given in previous section. Important numerical results obtained in optimization study are given in Figs. 7 and 8, which show the fiber orientation θ and the associated critical buckling pressure p_{cr} determined in each iteration for all shells. The initial values of θ are selected to be 0 deg for all composite shells. All the solutions converged within 11 or 12 iterations. Figure 9 shows the optimal fiber angles and the associated critical buckling pressure for all shells. From Fig. 9(a) we can
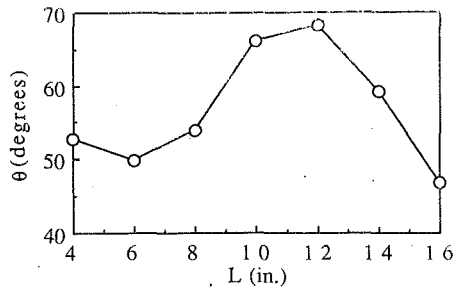
(a) Shell length L vs. optimal fiber orientation θ
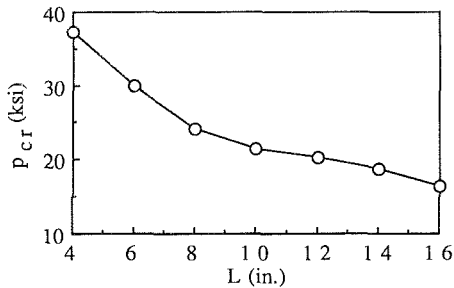
(b) Shell length L vs. critical pressure p_{cr}

Note: 1 in. = 2.54 cm; 1 ksi = 6.89 MPa

Fig. 9 Effect of shell length on buckling optimization of $[\pm\theta/90_2/0]_{10s}$ composite laminate shells under hydrostatic compression (simply supported ends)

Critical buckling mode for shell with L = 4 in. (10.16 cm)
$p_{cr} = 37.3$ ksi (257.0 MPa)

Critical buckling mode for shell with L = 16 in. (40.64 cm)
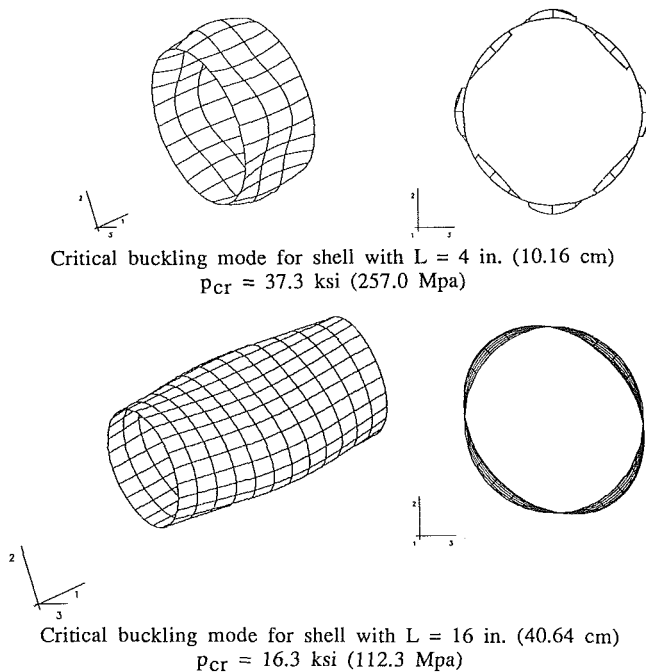$p_{cr} = 16.3$ ksi (112.3 MPa)

Fig. 10 Buckling modes of $[\pm\theta/90_2/0]_{10s}$ composite shells subjected to hydrostatic compression under optimal fiber orientation (simply supported ends)

see that for different shell lengths, the values of the optimal fiber angles vary between 46.7 and 68.1 deg and the optimal fiber angle θ seems to be a third-order function of shell length. From Fig. 9(b) we can see that when the length of the shell increases, the critical buckling pressure for composite shell under optimal fiber orientation decreases significantly. When shell length increases 4 times from 4 in. (10.16 cm) to 6 in. (40.64 cm), the critical buckling decreases 2.3 times from 37.3

ksi (257.0 MPa) to 16.3 ksi (112.3 MPa). Figure 10 shows the buckling modes of composite shells under optimal fiber angles with shell length L equal to 4 and 16 in. All these shells buckle into a single half-wave in the longitudinal direction. However, when the length of the shell section increases, the buckling mode of the composite shell develops less surface distortion in the circumferential direction.

Conclusions

From this optimization study of buckling of composite laminate cylindrical shells with different thickness and length, several important conclusions are obtained:

1 For composite shells with fixed length and with $[\pm\theta/90_2/0]_{nS}$ layup under external hydrostatic compression, the optimal fiber angle θ seems to be a second-order function of shell thickness. When the thickness of the shell section increases, the critical buckling pressure for composite shell under optimal fiber orientation increases significantly and the buckling mode of the shell develops less surface distortion in the circumferential direction.

2 For composite shells with fixed thickness and with $[\pm\theta/90_2/0]_{10S}$ layup under external hydrostatic compression, the optimal fiber angle θ seems to be a third-order function of shell length. When the length of the shell increases, the critical buckling pressure for composite shell under optimal fiber orientation decreases significantly and the buckling mode of the shell develops less surface distortion in the circumferential direction.

3 The structural dimensions have significant influence on the optimal fiber angle, critical buckling pressure and buckling mode of composite shells.

Acknowledgments

References

Bathe, K. J., and Wilson, E. J., 1972, "Large Eigenvalue Problems in Dynamic Analysis," *Journal of Engineering Mechanics Division*, ASCE, Vol. 98, pp. 1471-1485.

Cook, R. D., Malkus, D. S., and Plesha, M. E., 1989, *Concepts and Applications of Finite Element Analysis*, Third Edition, Chap. 14, John Wiley and Sons, New York.

Esping, B. J. D., 1984, "Minimum Weight Design of Membrane Structures," *Computers and Structures*, Vol. 19, pp. 707-716.

Hibbitt, Karlsson, and Sorensen, Inc., 1990, *ABAQUS User Manual*, Version 4-7, Providence, RI.

Hu, H.-T., and Wang, S. S., 1990, "Optimization for Buckling Resistance of Fiber-Composite Laminate Shells with and without Cutouts," *Proceedings of the 31st AIAA/ASME/ASCE/AHS/ASC Structures, Structural Dynamics and Materials Conference*, Long Beach, Calif., pp. 1300-1312.

Irons, B. M., 1976, "The Semi-Loof Shell Element," *Finite Elements for Thin Shells and Curved Members*, eds., D. G. Ashwell and R. H. Gallagher, John Wiley and Sons, London, pp. 197-222.

. Jun, S. M., and Hong, C. S., 1988, "Buckling Behavior of Laminated Composite Cylindrical Panels under Axial Compression," *Computers and Structures*, Vol. 29, pp. 479-490.

Knight, N. F., and Starnes, J. H., 1985, "Postbuckling Behavior of Axially Compressed Graphite-Epoxy Cylindrical Panels with Circular Holes," ASME JOURNAL OF PRESSURE VESSEL TECHNOLOGY, Vol. 107, pp. 394-402.

Kolmon, B., and Beck, R. E., 1980, *Elementary Linear Programming with Applications*, Chap. 2, Academic Press, Orlando, Fla.

Maror, M. J., 1987, *Numerical Analysis—A Practical Approach*, Chap. 2, Second Edition, Macmillan Publishing Company, New York.

Onoda, J., 1985, "Optimal Laminate Configurations of Cylindrical Shells for Axial Buckling," *AIAA Journal*, Vol. 23, pp. 1093-1098.

Schmit, L. A., 1981, "Structural Synthesis—Its Genesis and Development," *AIAA Journal*, Vol. 19, pp. 1249-1263.

Sun, G., and Hansen, J. S., 1988, "Optimal Design of Laminated-Composite Circular-Cylindrical Shells Subjected to Combined Loads," ASME *Journal of Applied Mechanics*, Vol. 55, pp. 136-142.

Vanderplaats, G. N., 1984, *Numerical Optimization Techniques for Engineering Design with Applications*, Chap. 6, McGraw-Hill, New York.

Whitney, J. M., 1984, "Buckling of Anisotropic Laminated Cylindrical Plates," *AIAA Journal*, Vol. 22, pp. 1641-1645.

Zienkiewicz, O. C., and Champbell, J. S., 1973, "Shape Optimization and Sequential Linear Programming," *Optimum Structural Design, Theory and Applications*, eds., R. H. Gallagher, and O. C. Zienkiewicz, John Wiley and Sons, New York, pp. 109-126.

APPENDIX

Constitutive Matrix for Fiber-Composite Laminae

During finite element analysis, the constitutive matrices of composite materials at element integration points must be calculated before the stiffness matrices are assembled from element level to global level. For fiber-composite laminate materials, each lamina can be considered as an orthotropic layer in a plane stress condition. The stress-strain relations for an orthotropic lamina in the material coordinates (Fig. 1) at an integration point can be written as

$$\{\sigma'\} = [Q_1']\{\epsilon'\} \tag{8}$$

$$\{\tau_t'\} = [Q_2']\{\gamma_t'\} \tag{9}$$

$$[Q_1'] = \begin{bmatrix} \dfrac{E_{11}}{1-\nu_{12}\nu_{21}} & \dfrac{\nu_{12}E_{22}}{1-\nu_{12}\nu_{21}} & 0 \\ \dfrac{\nu_{21}E_{11}}{1-\nu_{12}\nu_{21}} & \dfrac{E_{22}}{1-\nu_{12}\nu_{21}} & 0 \\ 0 & 0 & G_{12} \end{bmatrix} \tag{10}$$

$$[Q_2'] = \begin{bmatrix} \alpha_1 G_{13} & 0 \\ 0 & \alpha_2 G_{23} \end{bmatrix} \tag{11}$$

where $\{\sigma'\} = \{\sigma_1, \sigma_2, \tau_{12}\}^T$, $\{\tau_t'\} = \{\tau_{13}, \tau_{23}\}^T$, $\{\epsilon'\} = \{\epsilon_1, \epsilon_2, \gamma_{12}\}^T$, $\{\gamma_t'\} = \{\gamma_{13}, \gamma_{23}\}^T$. The α_1 and α_2 are shear correction factors and taken to be 0.83 in this study. The constitutive equations for the lamina in the element coordinates then become

$$\{\sigma\} = [Q_1]\{\epsilon\}, \qquad [Q_1] = [T_1]^T[Q_1'][T_1] \tag{12}$$

$$\{\tau_t\} = [Q_2]\{\gamma_t\}, \qquad [Q_2] = [T_2]^T[Q_2'][T_2] \tag{13}$$

$$[T_1] = \begin{bmatrix} \cos^2\phi & \sin^2\phi & \sin\phi\cos\phi \\ \sin^2\phi & \cos^2\phi & -\sin\phi\cos\phi \\ -2\sin\phi\cos\phi & 2\sin\phi\cos\phi & \cos^2\phi - \sin^2\phi \end{bmatrix} \tag{14}$$

$$[T_2] = \begin{bmatrix} \cos\phi & \sin\phi \\ -\sin\phi & \cos\phi \end{bmatrix} \tag{15}$$

where $\{\sigma\} = \{\sigma_x, \sigma_y, \tau_{xy}\}^T$, $\{\tau_t\} = \{\tau_{xz}, \tau_{yz}\}^T$, $\{\epsilon\} = \{\epsilon_x, \epsilon_y, \gamma_{xy}\}^T$, $\{\gamma_t\} = \{\gamma_{xz}, \gamma_{yz}\}^T$, and ϕ is measured counterclockwise from the element local x-axis to the material 1-axis. Assume $\{\epsilon_o\} = \{\epsilon_{xo}, \epsilon_{yo}, \gamma_{xyo}\}^T$ are the in-plane strains at the midsurface of the section and $\{\kappa\} = \{\kappa_x, \kappa_y, \kappa_{xy}\}^T$ are the curvatures. The in-plane strains at a distance, z, from the midsurface become

$$\{\epsilon\} = \{\epsilon_o\} + z\{\kappa\} \tag{16}$$

If h is the total thickness of the section, the stress resultants, $\{N\} = \{N_x, N_y, N_{xy}\}^T$, $\{M\} = \{M_x, M_y, M_{xy}\}^T$ and $\{V\} = \{V_x, V_y\}^T$, can be defined as

$$\{N\} = \int_{-h/2}^{h/2} \{\sigma\}dz = \int_{-h/2}^{h/2} [Q_1](\{\epsilon_o\} + z\{\kappa\})dz \tag{17}$$

$$\{M\} = \int_{-h/2}^{h/2} z\{\sigma\}dz = \int_{-h/2}^{h/2} z[Q_1](\{\epsilon_o\} + z\{\kappa\})dz \tag{18}$$

$$\{V\} = \int_{-h/2}^{h/2} \{\tau_t\}dz = \int_{-h/2}^{h/2} [Q_2]\{\gamma_t\}dz \tag{19}$$

If there are n layers in the layup, the foregoing equations can be rewritten as a summation of integrals over the n laminae in the following forms:

$$\begin{Bmatrix} \{N\} \\ \{M\} \\ \{V\} \end{Bmatrix} = \sum_{j=1}^{n} \begin{bmatrix} (z_{jt} - z_{jb})[Q_1] & \frac{1}{2}(z_{jt}^2 - z_{jb}^2)[Q_1] & [0] \\ \frac{1}{2}(z_{jt}^2 - z_{jb}^2)[Q_1] & \frac{1}{3}(z_{jt}^3 - z_{jb}^3)[Q_1] & [0] \\ [0]^T & [0]^T & (z_{jt} - z_{jb})[Q_2] \end{bmatrix} \begin{Bmatrix} \{\epsilon_o\} \\ \{\kappa\} \\ \{\gamma_t\} \end{Bmatrix} \tag{20}$$

where z_{jt} and z_{jb} are the distance from the mid-surface of the section to the top and the bottom of the jth layer, respectively. The [0] is a 3 by 2 matrix with all the coefficients equal to zero. It should be noted that for composite laminae with symmetic layup, the extensional and the flexural terms in the constitutive matrix (Eq. (20)) become uncoupled.